American Society of Hematology
2021 L Street NW, Suite 900,
Washington, DC 20036
Phone: 202-776-0544 | Fax 202-776-0545
editorial@hematology.org

# FGF trapping impairs multiple myeloma growth through c-Myc degradation-induced mitochondrial oxidative stress

Tracking no: BLD-2019-001310

Roberto Ronca (Brescia University), Gaia Ghedini (Brescia University), Federica Maccarinelli (Brescia University), Antonio Sacco (ASST Spedali Civili di Brescia), Silvia Laura Locatelli (Humanitas Cancer Center, Humanitas Clinical and Research Center), Eleonora Foglio (Brescia University), Sara Taranto (Brescia University), Elisabetta Grillo (Brescia University), Sara Matarazzo (Brescia University), Riccardo Castelli (University of Parma), Giuseppe Paganini (Brescia University), Vanessa Desantis (University of Bari), Nadia Cattane (IRCCS Istituto Centro San Giovanni di Dio Fatebenefratelli), Annamaria Cattaneo (IRCCS Istituto Centro San Giovanni di Dio Fatebenefratelli), Marco Mor (University of Parma), Carmelo Carlo-Stella (Istituto Clinico Humanitas IRCCS), Angelo Belotti (A.O. Spedali Civili), Aldo Roccaro (ASST Spedali Civili di Brescia), Marco Presta (University of Brescia), and Arianna Giacomini (Brescia University)

**Abstract:**
Multiple myeloma (MM), the second most common hematological malignancy, frequently relapses because of chemotherapeutic resistance. Fibroblast growth factors (FGFs) act as pro-angiogenic and mitogenic cytokines in MM. Here, we demonstrate that the autocrine FGF/FGFR axis is essential for MM cell survival and progression by protecting MM cells from oxidative stress-induced apoptosis. In keeping with the hypothesis that the intracellular redox status can be a target for cancer therapy, we show that extracellular FGF blockade by a FGF blocking approach based on a pan-FGF trap small molecule (NSC12) impairs the growth and dissemination of MM cells harbouring or not the t(4;14) translocation. NSC12 induces mitochondrial oxidative stress, DNA damage and apoptotic cell death in MM cells, prevented by the antioxidant vitamin E or mitochondrial catalase overexpression. Mitochondrial oxidative stress occurs as a consequence of proteasomal degradation of the c-Myc oncoprotein that leads to glutathione depletion. Accordingly, expression of a proteasome-non-degradable c-Myc protein mutant was sufficient to rescue the pro-apoptotic effects due to FGF blockade. These findings were confirmed on Bortezomib-resistant MM cells as well as on bone marrow-derived primary MM cells from newly diagnosed and relapsed/refractory patients, including plasma cells bearing the t(4;14) translocation obtained from high-risk MM patients. Altogether, our findings dissect for the first time the mechanism by which the FGF/FGFR system plays a non-redundant role in MM cell survival and disease progression, and indicate that FGF targeting may represent a therapeutic approach for MM patients with poor prognosis and advanced disease stage.

**Conflict of interest:** No COI declared

**COI notes:**

**Preprint server:** No;

**Author contributions and disclosures:** R.R. conceived in vitro and in vivo experiments, analysed the data and revised the manuscript; G.C.G. performed in vitro experiments; F.M. performed in vivo experiments; A.S. and S.L.L. isolated patient-derived MM cells and performed in vitro experiments; E.F. and S.T. performed in vitro experiments; E.G. performed seahorse experiments; S.M. performed in vitro experiments; R.C. synthetized NSC12; G.P. performed experiments with zebrafish; V.D. isolated patient-derived MM cells and performed in vitro experiments; N.C. and A.C. analysed GEP data; M.M. conceived NSC12 synthesis; C.C-S., A.B. and A.M.R. collected BM samples; M.P. conceived experiments and revised the manuscript; A.G. conceived and performed in vitro experiments, performed histological analyses, analysed the data and wrote the manuscript.

**Non-author contributions and disclosures:** No;

**Agreement to Share Publication-Related Data and Data Sharing Statement:** For original data, please contact arianna.giacomini@unibs.it. Microarray data are available at GEO under accession number GSE129279

**Clinical trial registration information (if any):**

# FGF trapping impairs multiple myeloma growth through c-Myc degradation-induced mitochondrial oxidative stress

Roberto Ronca[1], Gaia Cristina Ghedini[1], Federica Maccarinelli[1], Antonio Sacco[2], Silvia Laura Locatelli[3], Eleonora Foglio[1], Sara Taranto[1], Elisabetta Grillo[1], Sara Matarazzo[1], Riccardo Castelli[4], Giuseppe Paganini[1], Vanessa Desantis[5], Nadia Cattane[6], Annamaria Cattaneo[6,7], Marco Mor[4], Carmelo Carlo-Stella[3], Angelo Belotti[8], Aldo Maria Roccaro[2], Marco Presta[1]*, Arianna Giacomini[1]*

**Affiliations:**

[1] Department of Molecular and Translational Medicine, University of Brescia, Brescia, Italy.

[2] Clinical Research Development and Phase I Unit, CREA Laboratory, ASST Spedali Civili di Brescia, Brescia, Italy

[3] Department of Oncology and Hematology, Humanitas Cancer Center, Rozzano (MI), Italy

[4] Department of Food and Drug, University of Parma, Parma, Italy

[5] Department of Biomedical Sciences and Human Oncology, Azienda Ospedaliera Consorziale Universitaria Policlinico di Bari, Bari, Italy

[6] Biological Psychiatry Unit, IRCCS Istituto Centro San Giovanni di Dio Fatebenefratelli, Brescia, Italy

[7] Stress, Psychiatry and Immunology Laboratory, Department of Psychological Medicine, Institute of Psychiatry, King's College London, London, UK

[8] Department of Hematology, ASST Spedali Civili di Brescia, Brescia, Italy

*Correspondence: marco.presta@unibs.it; arianna.giacomini@unibs.it

**Running title:** FGF blockade triggers MM oxidative stress

**Text word count:** 3988
**Abstract word count:** 244
**Number of figures:** 7
**Number of tables:** 1
**Number of references:** 70

**Scientific category:** Lymphoid neoplasia

## KEY POINTS

- Autocrine FGF signaling protects MM cells from oxidative stress-induced apoptosis via c-Myc oncoprotein stabilization

- FGF blockade induces apoptosis of MM cells from drug-naive and relapsed/refractory patients, representing a novel therapeutic approach in MM

## ABSTRACT

Multiple myeloma (MM), the second most common hematological malignancy, frequently relapses because of chemotherapeutic resistance. Fibroblast growth factors (FGFs) act as pro-angiogenic and mitogenic cytokines in MM. Here, we demonstrate that the autocrine FGF/FGFR axis is essential for MM cell survival and progression by protecting MM cells from oxidative stress-induced apoptosis. In keeping with the hypothesis that the intracellular redox status can be a target for cancer therapy, we show that extracellular FGF blockade by a FGF blocking approach based on a pan-FGF trap small molecule (NSC12) impairs the growth and dissemination of MM cells harbouring or not the t(4;14) translocation. NSC12 induces mitochondrial oxidative stress, DNA damage and apoptotic cell death in MM cells, prevented by the antioxidant vitamin E or mitochondrial catalase overexpression. Mitochondrial oxidative stress occurs as a consequence of proteasomal degradation of the c-Myc oncoprotein that leads to glutathione depletion. Accordingly, expression of a proteasome-non-degradable c-Myc protein mutant was sufficient to rescue the pro-apoptotic effects due to FGF blockade. These findings were confirmed on Bortezomib-resistant MM cells as well as on bone marrow-derived primary MM cells from newly diagnosed and relapsed/refractory patients, including plasma cells bearing the t(4;14) translocation obtained from high-risk MM patients. Altogether, our findings dissect for the first time the mechanism by which the FGF/FGFR system plays a non-redundant role in MM cell survival and disease progression, and indicate that FGF targeting may represent a therapeutic approach for MM patients with poor prognosis and advanced disease stage.

**KEYWORDS**

Multiple myeloma, FGF/FGFR system, FGF trap, FGF inhibition, mitochondrial oxidative stress, c-Myc, proteasome

## INTRODUCTION

Multiple myeloma (MM) represents the second most common hematological malignancy[1] and is characterized by the clonal proliferation of malignant plasma cells within the bone marrow (BM).[2] MM relapses in the majority of patients because of chemotherapeutic resistance, indicating that novel biologically-based treatments are urgently required.

MM cells behavior is determined by their genetic background and cross-talk with the BM microenvironment which activates a pleiotropic cascade of proliferative/anti-apoptotic signaling pathways.[3,4] These events are triggered by the production of several growth factors by BM stromal cells (BMSCs) and/or MM cells in a paracrine/autocrine manner, leading to disease progression and drug resistance. In this frame, fibroblast growth factors (FGFs) play a pivotal role acting as potent pro-angiogenic mediators[5-8] and mitogenic cytokines.[9-11] Elevated levels of FGF2 are detectable in the BM and serum of MM patients and correlate with disease activity.[12-14] In addition, patient-derived MM cells secrete FGF2, representing the prevailing source in the BM of patients with active disease.[8,9]

The relevance of autocrine/paracrine FGF signaling in MM is supported by the observation that FGF receptors (FGFRs) are expressed by MM cell lines, patient-derived MM cells and within the BM milieu.[9,11,15] Also, FGFR3 has been implicated in MM cell proliferation and survival [16-20] and 15% of MM patients overexpress FGFR3 due to a t(4;14)(p16.3;q32) translocation.[21] Although a small fraction of these patients harbor a FGFR3 activating mutation, the majority of them upregulate the wild-type FGFR3 receptor, thus depending on FGF ligand for activation.[22] MM cells express various FGFs, including FGF2, regardless of FGFR3 up-regulation,[11,23] suggesting that autocrine FGF signaling may contribute to MM growth also independently from deregulated FGFR expression.

Altogether these findings make the FGF/FGFR system a promising target in MM therapy, and FGF inhibitors may exert a simultaneous “two compartment” effect by hampering autocrine/paracrine oncogenic signaling in MM.[24]

Recently, we have identified the PTX3-derived small molecule NSC12 as the first orally active pan-FGF trap able to inhibit FGFR activation and tumor growth in various FGF-dependent murine and human cancer models.[25,26] Notably, extracellular FGF traps, including NSC12, appear to be devoid of the toxicities associated to tyrosine kinase (TK) FGFR inhibitors, [26,27] thus representing a potential alternative to inhibit the FGF/FGFR system in MM.

Here, we dissected for the first time the mechanism by which the FGF/FGFR system plays a non-redundant role in MM cell survival and disease progression. Our findings reveal that FGF blockade by NSC12 triggers MM mitochondrial oxidative stress, DNA damage and apoptotic cell death *via*

the proteasomal degradation of the c-Myc oncoprotein. Our findings point to the FGF trapping approach as a promising therapeutic strategy for MM.

## MATERIALS AND METHODS

**Cell cultures and reagents.** KMS-11 and KMS-11/BTZ cells were obtained from the Japanese Collection of Research Bioresources (JCRB, Osaka, Japan) cell bank; RPMI8226, U-266, OPM-2 cells from the German Collection of Microorganisms and Cell Cultures (DSMZ, Braunschweig, Germany); MM.1S cells from ATCC (Manassas, VA, USA); GFP/Luciferase–expressing MM.1S cells were from Dr. Ghobrial, (Dana-Farber Cancer Institute, Boston, MA). All cell lines were maintained at low passage in RPMI1640 medium supplemented with 10% heat inactivated FBS and 2.0 mM glutamine, tested regularly for *Mycoplasma* negativity, and authenticated by PowerPlex Fusion System (Promega, Madison, USA).

For lentiviral transduction of KMS-11 cells, particles coding for the mitochondrial Catalase (pLVX-EF1a-IRES-puro-CatalaseMito),[28] the cytoplasmic Catalase (pLVX-IRES-neo-hCatalaseCito),[28] or the mutated Myc (Lenti-Myc T58A, Gentaur s.r.l, Bergamo, Italy) were used.

For details about the reagents used, see the reagent table in Supplemental Information.

**Cytofluorimetric analyses.** Cytofluorimetric analyses were performed using the MACSQuant® Analyzer (Miltenyi Biotec). Viable cell counting and cell cycle analyses were performed as described.[26] Mitochondrial membrane depolarization, mitochondrial (mt)ROS production and GSH levels were determined using the fluorescent probes tetramethylrhodamine ethyl ester (TMRE), Mitosox and ThiolTracker™ Violet (Thermo Fischer Scientific), respectively. Apoptotic cell death was assessed by Annexin-V/Iodide Propidium double staining (Immunostep) according to manufacturer's instructions.

**Western blot analysis.** Cells were washed in cold PBS and homogenized in NP-40 lysis buffer (1% NP-40, 20 mM Tris–HCl pH 8, 137 mM NaCl, 10% glycerol, 2 mM EDTA, 1 mM sodium orthovanadate, 10 μg/mL aprotinin, 10 μg/mL leupeptin). Protein concentration in the supernatants was determined using the Bradford protein assay (Bio-Rad Laboratories). Activation of signaling pathways and expression of specific proteins were detected using specific antibodies indicated in the reagent table in Supplemental Information.

For murine bone marrow analysis, femurs were explanted from mice systemically injected with GFP/Luciferase expressing MM.1S cells, flushed using PBS, and cells collected and processed as

indicated above. β-actin, α-tubulin or GAPDH were used as loading controls (see reagent table in Supplemental Information for antibodies details). Chemiluminescent signal was acquired by ChemiDoc™ Imaging System (BioRad) and analyzed using the ImageJ software (http://rsb.info.nih.gov/ij/).

**Human phospho-protein proteome profiler array.** Lysates (200 μg) from DMSO and NSC12-treated cells were incubated with the human phospho-kinase array kit (R&D Systems) according to manufacturer's instructions. Chemiluminescent signal was acquired and analyzed using the ImageJ software.

**Genome-wide expression profiling (GEP).** GEP was performed on cells treated with NSC12 (6 μM) for 6 or 12 hours, as reported in Supplemental Information. A cut-off of p-value < 0.01 (FDR corrected) and $Log_2$ fold change ± 2 was applied to select differentially expressed genes.

**RT-PCR and RT-qPCR.** Total RNA was extracted using TRIzol Reagent (Invitrogen) according to manufacturer's instructions. Two μg of total RNA were retro-transcribed with MMLV reverse transcriptase (Invitrogen) using random hexaprimers. Then, cDNA was analysed by semiquantitative or quantitative PCR using primers indicated in the reagent table in Supplemental Information.

**Seahorse analysis.** KMS-11 cells were seeded at $4x10^5$ cells/well on Seahorse XFe24 culture plates (Agilent) previously treated with 3.5 μg/$cm^2$ Corning™ Cell-Tak Cell and Tissue Adhesive. Oxygen consumption rate (OCR) and extracellular acidification rate (ECAR) measurements were performed using a Seahorse XFe24 Extracellular Flux Analyzer (XFe Wave software). For further details see Supplemental Information.

**Subcutaneous human xenografts**. Experiments were performed according to the Italian laws (D.L. 116/92 and following additions) that enforce the EU 86/109 Directive and were approved by the Institutional Ethical Committee for Animal Experimentation.
Six- to eight-week old female NOD/SCID mice (Envigo, Udine, Italy) were injected subcutaneously (s.c.) with KMS-11 and RPMI8226 cells ($5x10^6$ cells/mouse) in 200 μl of PBS. When tumors were palpable, mice were randomly assigned to receive daily treatment with NSC12 (7.5 mg/kg) or control/vehicle DMSO. For further details see Supplemental Information.

**Systemic human xenograft.** Six- to eight-week old female SCID Beige mice (Envigo) were injected intravenously (i.v) with GFP/Luciferase expressing MM.1S cells ($2x10^6$ cells/mouse) in 100 µl of PBS. Mice were randomly assigned to receive short- or long-term i.p. treatments with NSC12 (7.5 mg/kg) or control/vehicle DMSO. For further details see Supplemental Information.

**Cytological and histological analyses**. Cytospin from patient-derived MM cells were prepared using about $2x10^5$ cells/slide. Tumor samples were either embedded in OCT compound and immediately frozen or fixed in formalin and embedded in paraffin. All samples were further processed as reported in Supplemental Information.

**Zebrafish embryo homing model.** The model was used as described.[29] Briefly, MM.1S cells were exposed for 3 hours to NSC12 3 µM or DMSO. Thirty minutes before the end of treatment, CMTPX or CMF2HC CellTracker™ dyes (Thermo Fisher Scientific) were added to cell suspensions to obtain fluorescently labelled red (NSC12-treated) or blue (DMSO-treated) MM.1S cells, respectively. After staining, NSC12- and DMSO-treated cells were washed, mixed together at a 1:1 ratio, and co-injected in the bloodstream of zebrafish embryos by the duct of Cuvier. Zebrafish experiments were performed as approved by the Institutional Ethical Committee for Animal Experimentation. For further details see Supplemental Information.

**Patient-derived MM cells.** This study was approved by the Institutional Review Board at Humanitas Cancer Center of Rozzano (Milan). Informed consent was obtained from all patients. Primary $CD138^+$ cells were obtained from freshly isolated MM patients' BM using $CD138^+$ microbeads selection, as reported.[30]

**Statistical analyses.** Statistical analyses were performed using Prism 6 (GraphPad Software). Student's *t* test for unpaired data (2-tailed) was used to test the probability of significant differences between two groups of samples. For more than two groups of samples, data were analyzed with a 1-way analysis of variance and corrected by the Bonferroni multiple comparison test. Tumor volume data were analyzed with a 2-way analysis of variance and corrected by the Bonferroni test. Differences were considered significant when $p< 0.05$ unless otherwise specified.

**Data sharing statement.** For original data, please contact arianna.giacomini@unibs.it. Microarray data are available at GEO under accession number GSE129279.

## RESULTS

### Inhibition of FGF/FGFR signaling triggers apoptosis of MM cells.

The human MM cell lines harbouring (KMS-11 and OPM-2 cells) or not (RPMI8226 and U-266 cells) the t(4;14) translocation express different FGFs and FGFRs (**Figure S1A)**. Autocrine activation of the FGF/FGFR system in these cells was confirmed by FGFR/FRS2 phosphorylation that occurs in the absence of exogenous stimuli (**Figure S1A**). When treated with the pan-FGF trap NSC12,[25,26] t(4;14)-positive and t(4;14)-negative MM cells showed impaired cell proliferation and survival, with alterations of cell cycle **(Figure 1A-C)**. Both KMS-11 and RPMI8226 cells showed a significant increase of apoptotic cells 6 hours after NSC12 treatment with 100% cell death at 24 hours (**Figures 1C and S1B**). Accordingly, NSC12 inhibited FGFR3 phosphorylation, activation of MAPK, Akt and JAK/STAT3 pathways and reduced the levels of the anti-apoptotic protein mcl-1, leading to the activation of caspase 3 in both cell lines (**Figure 1D**). Similar results were obtained after treatment with the TK FGFR inhibitor BGJ398 (**Figure S1C-E**). A significant reduction of MM cell survival was observed also when KMS-11 cells were co-cultured with patient-derived BMSCs and treated with NSC12, suggesting that FGF trapping might disrupt FGF-mediated BMSC/MM cell cross/talk (**Figure S1F-G**).

In keeping with the *in vitro* observations, oral treatment with NSC12 caused a significant inhibition of FGFR3 phosphorylation **(Figure 2A)** and tumor growth when KMS-11 and RPMI8226 cells were grafted s.c. in immunodeficient mice (**Figure 2B)**. This was accompanied by inhibition of tumor cell proliferation and increased apoptosis, as revealed by phospho-Histone H3 and TUNEL immunostaining, respectively (**Figure 2C)**. In keeping with the role of the FGF/FGFR system in tumor angiogenesis, NSC12-treated tumors showed also a decrease in $CD31^+$ vascularization (**Figure S1H)**.

### FGF trapping inhibits MM dissemination.

The MM.1S cell line represents an experimental platform suitable for the study of MM dissemination *in vivo*.[31,32] MM.1S cells express all four FGFRs and FGF2/3/9 (**Figure S1A**). NSC12 administration hampered FGFR1 and FGFR3 phosphorylation also in these cells (**Figure 3A**), thus inhibiting their proliferation and increasing the number of apoptotic cells at 6 hours after treatment onward (**Figure 3B**). Notably, NSC12-treated cells were characterized by a decreased capacity to migrate towards chemotactic stimuli represented by FBS or the SDF1α chemokine **(Figure 3C**). FAK kinase and β-catenin are regulated by FGF/FGFR signaling[33-36] and support the migration and adhesion of MM cells in the BM niche.[37,38] Accordingly, NSC12 strongly reduced

FAK phosphorylation and the levels of FAK and β-catenin in MM.1S cells (**Figure 3D**), indicating a link between the FGF/FGFR axis and MM cell migration.

To investigate whether NSC12 might affect the homing of MM cells to the BM, we took advantage of a zebrafish embryo model in which the caudal hematopoietic tissue (CHT) recapitulates a BM-like niche.[29] MM.1S cells were stained with a red or blue fluorescent dye and treated with vehicle (DMSO) or NSC12, respectively. After 3 hours, an incubation time that does not cause MM.1S cell death, the two cell preparations were mixed together (1:1 ratio) and co-injected in the bloodstream of zebrafish embryos (**Figure 3E**). As shown in **Figure 3F**, NSC12 pre-treatment significantly prevented MM cell homing to the CHT when compared to DMSO-treated cells.

Next, GFP/luciferase-expressing MM.1S cells were systemically injected in SCID beige mice. BM infiltration was detectable 2 weeks after injection and reached a peak after 6-8 weeks, when approximately 40% of the BM cell population was represented by tumor cells (**Figure 3G**). On this basis, mice bearing 10-20% of MM.1S cell BM colonization/infiltration were treated for three days with NSC12. BM analysis showed that NSC12 reduced the levels of phosphorylated FGFR3 in NSC12-treated mice to those detected in disease-free animals **(Figure 3H**). Accordingly, chronic NSC12 treatment significantly reduced BM tumor burden in MM.1S cell-grafted animals (**Figure 3I**). Together, these data indicate that NSC12 inhibits FGF/FGFR signaling and proliferation of MM cells growing within their own microenvironment.

**Inhibition of FGF signaling induces oxidative stress-mediated DNA damage and apoptosis in MM cells.**

To get further insights into the impact of FGF inhibition in MM, gene expression profiling (GEP) analysis was performed on NSC12-treated KMS-11 cells. The analysis revealed a significant $Log_2$ 2-fold upregulation of 33 and 44 genes after 6 and 12 hours of treatment, respectively (**Figure 4A, Figure S2A**), the majority of them being related to oxidative stress and DNA damage (**Table S1, Figure S2B**). Accordingly, phospho-kinase array analysis showed the activation of oxidative stress and DNA damage-induced protein kinases and confirmed the inactivation of Akt, Erk and STAT kinases as well as reduced levels of FAK and β-catenin phosphorylation (**Figure S2C**). Together, these data suggest that the autocrine FGF/FGFR axis may play a role in preventing oxidative stress and consequent DNA damage in MM cells.

In keeping with this hypothesis, NSC12 rapidly increased mtROS production and mitochondrial membrane depolarization in KMS-11 (**Figure 4B**) and RPMI8226 (**Figure S2D**) cells. mtROS production was paralleled by PARP inactivation and extensive DNA damage, as assessed by increased levels of phospho-H2AX (γH2AX) (**Figure 4C**). Accordingly, NSC12 caused a strong

reduction of mitochondrial respiration 1 hour after treatment and a complete dysfunction of mitochondrial activity 3 hours thereafter, leading to mitochondrial proton leak and medium acidification (**Figures 4D and S2E**). Oxidative stress and DNA damage were observed also in tumor xenografts treated with NSC12, as assessed by anti-nitro tyrosine and anti-pH2AX staining, respectively (**Figure 4E**). Notably, administration of the antioxidant vitamin E[39] prevented NSC12-induced mtROS production, mitochondrial depolarization, DNA damage and apoptosis in MM cells (**Figures 4F-G and S2F**) without affecting the capacity of the compound to inhibit FGFR phosphorylation (**Figure 4G**). Accordingly, overexpression of mitochondrial catalase[28], but not cytoplasmic catalase, significantly reduced mtROS production and cell death in NSC12-treated KMS-11 cells (**Figure S2G**). Finally, vitamin E exerted a rescue effect also when FGFR signaling was inhibited by the TK FGFR inhibitor BGJ398 (**Figure S2F**). Together, these data highlight the capacity of the autocrine FGF/FGFR axis to prevent mitochondrial oxidative stress, thus allowing cell survival in MM.

**c-Myc degradation mediates oxidative stress and apoptosis induced by FGF inhibition in MM cells.**

In order to understand the mechanism by which the inhibition of FGF signaling triggers oxidative stress-induced cell death in MM, GSEA of GEP data was performed on NSC12-treated KMS-11 cells. In agreement with the impact of NSC12 on MM cell proliferation/survival and migration, GSEA showed the enrichment of mitotic spindle, G2/M checkpoint and wnt/β-catenin signaling hallmarks that were significantly down-modulated after NSC12 treatment (**Figure S3A**). GSEA revealed also the down-modulation of c-Myc targets (**Figure 5A**), confirmed by RT-qPCR (**Figure S3B**). Accordingly, a rapid disappearance of c-Myc protein occurred in MM cells after NSC12 treatment **(Figures 5B and S3C)** in the absence of significant changes of *c-MYC* mRNA levels at 3 and 6 hours of NSC12 treatment (**Figure S3D**), suggesting that FGF inhibition may induce proteasomal degradation of c-Myc protein. Indeed, the proteasome inhibitor MG132 prevented c-Myc protein degradation triggered by NSC12 in KMS-11 cells (**Figure 5C**).

GSK3αβ kinase is a FGFR-mediated modulator of proteasomal c-Myc degradation.[33,40-43] NSC12 inhibited GSK3αβ kinase phosphorylation, leading to the activation of this kinase (**Figure 5B**).[44] A significant reduction of c-Myc and phospho-GSK3αβ kinase levels was observed also in NSC12-treated KMS-11 tumor xenografts (**Figure 5B**), suggesting that GSK3αβ kinase activation following FGF trapping may induce c-Myc proteasomal degradation, leading to down-regulation of c-Myc target genes.

To assess the role of c-Myc degradation in oxidative stress and apoptosis induced by FGF inhibition in MM cells, we generated KMS-11 cells overexpressing the undegradable T58A mutant form of c-Myc.[45,46] Ectopic expression of the c-Myc$^{(T58A)}$ mutant prevented NSC12-induced c-Myc degradation (**Figure 5D**) and blocked NSC12-induced production of mtROS, thus preserving MM cells from apoptosis (**Figure 5E**).

The intracellular content of the anti-oxidant glutathione (GSH) is depleted upon c-Myc down-regulation, thus mediating c-Myc-dependent drug-induced apoptosis.[47] Accordingly, GSH levels were strongly reduced in NSC12-treated KMS-11 (**Figure 5F**) and RPMI8226 (**Figure S3E**) cells, but not in Myc$^{(T58A)}$ KMS-11 cells (**Figure 5G**). Notably, vitamin E did not significantly prevent GSH depletion upon treatment with NSC12 (**Figure 5H**), suggesting that GSH depletion might represent an upstream event in the oxidative stress cascade triggered by c-Myc degradation following inhibition of the autocrine FGF/FGFR system in MM cells.

**NSC12 induces oxidative stress and cell death in newly diagnosed and refractory/relapsed patient-derived MM cells.**

To assess the therapeutic implications consequent to FGF inhibition in MM, tumor cells freshly isolated from 26 MM patients (**Table 1**) were treated with NSC12 and assessed for cell death. Twenty-two cases responded to NSC12 regardless of t(4;14) translocation (**Figure 6A, Tables 1**). Interestingly, NSC12 was efficacious in both newly diagnosed (10/10) and refractory/relapsed (12/16) patients (**Table 1**). In both cases, western blot analysis showed a strong inhibition of FGFR3, $ERK_{1/2}$, JAK2 and STAT3 phosphorylation, reduction of mcl-1 levels, and caspase 3 activation (**Figure 6B**). Only a limited effect, in the absence of caspase 3 activation (**Figure S4**), was exerted by the highest dose of NSC12 on PBMCs isolated from eight healthy donors, being totally ineffective at lower doses (**Figure 6A**).

As observed for MM cell lines, NSC12 caused a drastic reduction of c-Myc protein from both newly diagnosed and relapsed/refractory patients (**Figure 6C**), paralleled by increased oxidative stress and DNA damage, as assessed by RT-qPCR analysis (**Figure 6D**) and anti-nitro tyrosine and phospho-H2AX staining (**Figure 6E**). Again, vitamin E rescued patient-derived MM cells from NSC12-induced cell death (**Figure 6F**).

Notably, no significant differences in NSC12 sensitivity were observed between MM cells from refractory/relapsed or newly diagnosed patients (**Figure 7A**). Accordingly, Bortezomib-resistant KMS-11/BTZ cells[48] responded *in vitro* and *in vivo* to NSC12 treatment in a manner similar to parental KMS-11 cells (**Figures 7B-E**), suggesting that FGF trapping may represent a therapeutic approach for MM cases relapsed from or not responding to proteasome inhibitor-based treatments.

In this frame, GEP (**Table S1**) and RT-qPCR (**Figure 7F**) analyses revealed a significant down-regulation of *TXNDC5* and of the c-Myc target *PRDX3* genes in NSC12-treated KMS-11 and KMS-11/BTZ cells (**Figure 7F**). The two genes are involved in the protection from oxidative stress and Bortezomib resistance in refractory/relapsed MM.[49] Altogether, these findings indicate that inhibition of the FGF/FGFR system may represent a promising approach to eradicate Bortezomib-refractory MM cells.

## DISCUSSION

Here we show for the first time that autocrine FGF/FGFR signaling protects MM cells from oxidative stress-induced apoptosis, thus playing a non-redundant role in MM cell survival. Based on a FGF trapping approach, we demonstrate that FGF blockade induces the degradation of the oncoprotein c-Myc; this causes GSH depletion and triggers mitochondrial oxidative stress, DNA damage and apoptosis in MM cells.

NSC12 acts as an extracellular pan FGF trap, exerting an oncosuppressive activity on FGF-dependent solid tumors.[25,26] Here, we demonstrate that NSC12 blocks MM cell proliferation and induces oxidative stress-dependent MM apoptotic cell death in both t(4;14)-positive and t(4;14)-negative MM cells. Notably, NSC12 causes a significant inhibition of MM cell survival also when MM cells are co-cultured with patient-derived BMSCs, suggesting that FGF trapping may disrupt FGF-mediated MM/BMS cells cross-talk. Accordingly, NSC12 inhibited the activation of FGF/FGFR signaling in MM cells growing in their own microenvironment after BM colonization and reduced BM tumor burden, pointing to a non-redundant role of the FGF/FGFR system in MM dissemination. In keeping with this hypothesis, NSC12 affected MM cell migration by reducing FAK activation and β-catenin protein levels and hampered MM cell homing to the zebrafish embryo BM-like niche.

GEP and phospho-protein array analyses demonstrated a significant increase of gene expression and protein phosphorylation events associated to oxidative stress and DNA damage in NSC12-treated KMS-11 cells. Accordingly, NSC12 rapidly increased mtROS production, membrane depolarization and mitochondrial dysfunction, paralleled by PARP inactivation and extensive DNA damage. This was prevented by the antioxidant vitamin E or mitochondrial catalase overexpression, indicating that mitochondrial oxidative stress is directly responsible for MM cell apoptosis upon FGF inhibition.

Oxidative stress-inducing agents have been approved for the treatment of solid malignancies and various types of leukemias and lymphomas.[50] Several evidences suggest that affecting the

intracellular redox status may represent a promising strategy also in MM. Indeed, elevated serum levels of oxidative stress markers are found in MM patients.[51-53] In addition, upregulation of the antioxidant superoxide dismutase-1 and epigenetic silencing of the oxidative stress sensitizer glutathione peroxidase 3 gene are associated to MM progression and poor prognosis.[54,55] Also, the small nucleolar RNA ACA11 inhibits oxidative stress and is overexpressed in patient-derived t(4;14)-positive MM cells.[56] Altogether, these findings indicate that the induction of ROS production by FGF/FGFR inhibitors may represent a novel anti-MM approach and suggest that the use of antioxidant supplements[57] in the context of FGF/FGFR inhibitory therapies should be carefully evaluated.

In keeping with data obtained from FGFR1 fusion-driven hematological malignancies[58], we observed a significant down-modulation of c-Myc targets after FGF inhibition in MM cells. Accordingly, NSC12 induced the degradation of c-Myc protein that was inhibited by the proteasome inhibitor MG132. This was paralleled by activation of GSK3αβ kinase, a direct regulator of c-Myc degradation.[40-42] In addition, ectopic expression of the undegradable c-Myc$^{(T58A)}$ mutant[45] prevented NSC12-induced mtROS production and apoptosis in KMS-11 cells. Together, these findings point to a direct link between FGF signaling, c-Myc activity and cell survival in MM. c-Myc controls mitochondrial metabolism and homeostasis[59] and upregulates the levels of mitochondrial glutaminase, leading to GSH synthesis.[60] GSH prevents apoptosis due to ROS production consequent to redox imbalance or enhanced mitochondrial function in response to increased c-Myc activity.[61,62] In keeping with these findings, recent evidences suggest that a large fraction of primary MM cells depends on c-Myc activity for survival.[63-65] Our data show that FGF trapping causes a significant depletion of GSH levels in wild type KMS-11 cells but not in Myc$^{(T58A)}$ mutants. This indicates that FGF/FGFR signaling protects MM cells from oxidative stress-mediated apoptosis through c-Myc-dependent regulation of GSH levels.

Our findings were confirmed within the clinical setting using primary BM-derived plasma cells from MM patients. Twenty-two out of the 26 cases examined responded significantly to NSC12 treatment regardless of t(4;14) chromosomal translocation. In agreement with the data obtained with MM cell lines, NSC12 treatment induced c-Myc degradation, ROS production and cell death that was prevented by the antioxidant vitamin E. These data confirm the pivotal role played by FGF autocrine/paracrine stimulation in MM and suggest FGF traps might represent a promising therapeutic approach in MM, including high-risk MM patients with the t(4;14) translocation.

Notably, NSC12 reduced c-Myc protein levels and increased oxidative stress also in MM primary cells obtained from patients with relapsed/refractory disease. Accordingly, NSC12 treatment exerts a similar oncosuppressive effect on both Bortezomib-resistant KMS-11/BTZ[48] and parental KMS-

11 cells *in vitro* and *in vivo*, with inhibition of the expression of *TXNDC5* and the c-Myc target *PRDX3*, both involved in the protection from oxidative stress and Bortezomib resistance in refractory/relapsed MM.[49] Together with previous observations showing that perturbation of mitochondrial function may decrease the resistance of MM cells to Bortezomib,[66] these findings suggest that molecules able to induce mitochondrial oxidative stress, including FGF/FGFR inhibitors, may represent a promising approach to eradicate proteasome inhibitor-relapsed/refractory cancer cells.

Four out of the 26 patient-derived MM cell cases tested showed a limited or no response to NSC12 treatment. Our data point to c-Myc as a key downstream effector able to determine the therapeutic response to FGF/FGFR inhibitors in MM. Upregulation of c-Myc protein is related to MM disease initiation and progression, being activated in a large fraction of MM patients.[67-70] Even though the presence of point mutations encoding for undegradable forms of c-Myc has not been reported for MM,[69] recent observations have shown that PKC-dependent phosphorylation of GSK3αβ kinase causes its inactivation in gastric cancer,[43] thus representing a possible mechanism of resistance/escape to anti-FGF therapies. Further studies will be required to get a deeper insight into the molecular mechanisms that allow or hamper the response to therapeutic approaches targeting the FGF/FGFR system in MM.

**ACKNOWLEDGMENTS**

This work was supported by grants from Fondazione Cariplo (grant n° 2016-0570) to A.G, Fondazione Regionale per la Ricerca Biomedica (FRRB, grant n° 2016-065 ERA-NET TRANSCAN-2) to A.M.R. and to C.C.-S. (FRRB, grant n° 2015-0042) and Associazione Italiana Ricerca sul Cancro to M.P. (AIRC grant n° 18943), R.R. (AIRC grant n° MFAG 18459) and C.C.-S. (AIRC grant n° 20575). E.G. and S.M. were supported by Fondazione Italiana per la Ricerca sul Cancro Fellowships and F.M. by a Fondazione Veronesi Fellowship.

The authors are grateful to Daniela Uberti and Mattia Bugatti for technical support.

**AUTHOR CONTRIBUTIONS**

R.R. conceived in vitro and in vivo experiments, analysed the data and revised the manuscript; G.C.G. performed in vitro experiments; F.M. performed in vivo experiments; A.S. and S.L.L. isolated patient-derived MM cells and performed in vitro experiments; E.F. and S.T. performed in vitro experiments; E.G. performed seahorse experiments; S.M. performed in vitro experiments; R.C. synthetized NSC12; G.P. performed experiments with zebrafish; V.D. isolated patient-derived MM cells and performed in vitro experiments; N.C. and A.C. analysed GEP data; M.M. conceived NSC12 synthesis; C.C-S., A.B. and A.R. collected BM samples; M.P. conceived experiments and revised the manuscript; A.G. conceived and performed in vitro experiments, performed histological analyses, analysed the data and wrote the manuscript.

**DECLARATION OF INTERESTS**

The authors declare no competing interests

**REFERENCES**

1. Siegel R, Naishadham D, Jemal A. Cancer statistics, 2013. *CA Cancer J Clin*. 2013;63(1):11-30.
2. Raab MS, Podar K, Breitkreutz I, Richardson PG, Anderson KC. Multiple myeloma. *Lancet*. 2009;374(9686):324-339.
3. Bommert K, Bargou RC, Stuhmer T. Signalling and survival pathways in multiple myeloma. *Eur J Cancer*. 2006;42(11):1574-1580.
4. van de Donk NW, Lokhorst HM, Bloem AC. Growth factors and antiapoptotic signaling pathways in multiple myeloma. *Leukemia*. 2005;19(12):2177-2185.
5. Ria R, Reale A, De Luisi A, Ferrucci A, Moschetta M, Vacca A. Bone marrow angiogenesis and progression in multiple myeloma. *Am J Blood Res*. 2011;1(1):76-89.
6. Ribatti D, Vacca A. New Insights in Anti-Angiogenesis in Multiple Myeloma. *Int J Mol Sci*. 2018;19(7).
7. Vacca A, Ribatti D, Roccaro AM, Frigeri A, Dammacco F. Bone marrow angiogenesis in patients with active multiple myeloma. *Semin Oncol*. 2001;28(6):543-550.

8. Vacca A, Ribatti D, Presta M, et al. Bone marrow neovascularization, plasma cell angiogenic potential, and matrix metalloproteinase-2 secretion parallel progression of human multiple myeloma. *Blood*. 1999;93(9):3064-3073.
9. Bisping G, Leo R, Wenning D, et al. Paracrine interactions of basic fibroblast growth factor and interleukin-6 in multiple myeloma. *Blood*. 2003;101(7):2775-2783.
10. Lentzsch S, Chatterjee M, Gries M, et al. PI3-K/AKT/FKHR and MAPK signaling cascades are redundantly stimulated by a variety of cytokines and contribute independently to proliferation and survival of multiple myeloma cells. *Leukemia*. 2004;18(11):1883-1890.
11. Otsuki T, Yamada O, Yata K, et al. Expression of fibroblast growth factor and FGF-receptor family genes in human myeloma cells, including lines possessing t(4;14)(q16.3;q32. 3) and FGFR3 translocation. *Int J Oncol*. 1999;15(6):1205-1212.
12. Di Raimondo F, Azzaro MP, Palumbo G, et al. Angiogenic factors in multiple myeloma: higher levels in bone marrow than in peripheral blood. *Haematologica*. 2000;85(8):800-805.
13. Sato N, Hattori Y, Wenlin D, et al. Elevated level of plasma basic fibroblast growth factor in multiple myeloma correlates with increased disease activity. *Jpn J Cancer Res*. 2002;93(4):459-466.
14. Sezer O, Jakob C, Eucker J, et al. Serum levels of the angiogenic cytokines basic fibroblast growth factor (bFGF), vascular endothelial growth factor (VEGF) and hepatocyte growth factor (HGF) in multiple myeloma. *Eur J Haematol*. 2001;66(2):83-88.
15. Walsh S, Jefferiss C, Stewart K, Jordan GR, Screen J, Beresford JN. Expression of the developmental markers STRO-1 and alkaline phosphatase in cultures of human marrow stromal cells: regulation by fibroblast growth factor (FGF)-2 and relationship to the expression of FGF receptors 1-4. *Bone*. 2000;27(2):185-195.
16. Plowright EE, Li Z, Bergsagel PL, et al. Ectopic expression of fibroblast growth factor receptor 3 promotes myeloma cell proliferation and prevents apoptosis. *Blood*. 2000;95(3):992-998.
17. Grand EK, Chase AJ, Heath C, Rahemtulla A, Cross NC. Targeting FGFR3 in multiple myeloma: inhibition of t(4;14)-positive cells by SU5402 and PD173074. *Leukemia*. 2004;18(5):962-966.
18. Trudel S, Ely S, Farooqi Y, et al. Inhibition of fibroblast growth factor receptor 3 induces differentiation and apoptosis in t(4;14) myeloma. *Blood*. 2004;103(9):3521-3528.
19. Trudel S, Li ZH, Wei E, et al. CHIR-258, a novel, multitargeted tyrosine kinase inhibitor for the potential treatment of t(4;14) multiple myeloma. *Blood*. 2005;105(7):2941-2948.
20. Trudel S, Stewart AK, Rom E, et al. The inhibitory anti-FGFR3 antibody, PRO-001, is cytotoxic to t(4;14) multiple myeloma cells. *Blood*. 2006;107(10):4039-4046.
21. Kalff A, Spencer A. The t(4;14) translocation and FGFR3 overexpression in multiple myeloma: prognostic implications and current clinical strategies. *Blood Cancer J*. 2012;2:e89.
22. Intini D, Baldini L, Fabris S, et al. Analysis of FGFR3 gene mutations in multiple myeloma patients with t(4;14). *Br J Haematol*. 2001;114(2):362-364.
23. Krejci P, Mekikian PB, Wilcox WR. The fibroblast growth factors in multiple myeloma. *Leukemia*. 2006;20(6):1165-1168.
24. Giacomini A, Chiodelli P, Matarazzo S, Rusnati M, Presta M, Ronca R. Blocking the FGF/FGFR system as a "two-compartment" antiangiogenic/antitumor approach in cancer therapy. *Pharmacol Res*. 2016;107:172-185.
25. Castelli R, Giacomini A, Anselmi M, et al. Synthesis, Structural Elucidation, and Biological Evaluation of NSC12, an Orally Available Fibroblast Growth Factor (FGF) Ligand Trap for the Treatment of FGF-Dependent Lung Tumors. *J Med Chem*. 2016;59(10):4651-4663.
26. Ronca R, Giacomini A, Di Salle E, et al. Long-Pentraxin 3 Derivative as a Small-Molecule FGF Trap for Cancer Therapy. *Cancer Cell*. 2015;28(2):225-239.
27. Bono F, De Smet F, Herbert C, et al. Inhibition of tumor angiogenesis and growth by a small-molecule multi-FGF receptor blocker with allosteric properties. *Cancer Cell*. 2013;23(4):477-488.

28. Gurgul E, Lortz S, Tiedge M, Jorns A, Lenzen S. Mitochondrial catalase overexpression protects insulin-producing cells against toxicity of reactive oxygen species and proinflammatory cytokines. *Diabetes*. 2004;53(9):2271-2280.
29. Sacco A, Roccaro AM, Ma D, et al. Cancer Cell Dissemination and Homing to the Bone Marrow in a Zebrafish Model. *Cancer Res*. 2016;76(2):463-471.
30. Roccaro AM, Mishima Y, Sacco A, et al. CXCR4 Regulates Extra-Medullary Myeloma through Epithelial-Mesenchymal-Transition-like Transcriptional Activation. *Cell Rep*. 2015;12(4):622-635.
31. Greenstein S, Krett NL, Kurosawa Y, et al. Characterization of the MM.1 human multiple myeloma (MM) cell lines: a model system to elucidate the characteristics, behavior, and signaling of steroid-sensitive and -resistant MM cells. *Exp Hematol*. 2003;31(4):271-282.
32. Lwin ST, Edwards CM, Silbermann R. Preclinical animal models of multiple myeloma. *Bonekey Rep*. 2016;5:772.
33. Hashimoto M, Sagara Y, Langford D, et al. Fibroblast growth factor 1 regulates signaling via the glycogen synthase kinase-3beta pathway. Implications for neuroprotection. *J Biol Chem*. 2002;277(36):32985-32991.
34. Hunger-Glaser I, Fan RS, Perez-Salazar E, Rozengurt E. PDGF and FGF induce focal adhesion kinase (FAK) phosphorylation at Ser-910: dissociation from Tyr-397 phosphorylation and requirement for ERK activation. *J Cell Physiol*. 2004;200(2):213-222.
35. Katoh M, Katoh M. Cross-talk of WNT and FGF signaling pathways at GSK3beta to regulate beta-catenin and SNAIL signaling cascades. *Cancer Biol Ther*. 2006;5(9):1059-1064.
36. Mavila N, James D, Utley S, et al. Fibroblast growth factor receptor-mediated activation of AKT-beta-catenin-CBP pathway regulates survival and proliferation of murine hepatoblasts and hepatic tumor initiating stem cells. *PLoS One*. 2012;7(11):e50401.
37. Qiang YW, Walsh K, Yao L, et al. Wnts induce migration and invasion of myeloma plasma cells. *Blood*. 2005;106(5):1786-1793.
38. Park SY, Wolfram P, Canty K, et al. Focal adhesion kinase regulates the localization and retention of pro-B cells in bone marrow microenvironments. *J Immunol*. 2013;190(3):1094-1102.
39. Traber MG, Atkinson J. Vitamin E, antioxidant and nothing more. *Free Radic Biol Med*. 2007;43(1):4-15.
40. Henriksson M, Bakardjiev A, Klein G, Luscher B. Phosphorylation sites mapping in the N-terminal domain of c-myc modulate its transforming potential. *Oncogene*. 1993;8(12):3199-3209.
41. Robertson H, Hayes JD, Sutherland C. A partnership with the proteasome; the destructive nature of GSK3. *Biochem Pharmacol*. 2018;147:77-92.
42. Welcker M, Orian A, Jin J, et al. The Fbw7 tumor suppressor regulates glycogen synthase kinase 3 phosphorylation-dependent c-Myc protein degradation. *Proc Natl Acad Sci U S A*. 2004;101(24):9085-9090.
43. Lau WM, Teng E, Huang KK, et al. Acquired Resistance to FGFR Inhibitor in Diffuse-Type Gastric Cancer through an AKT-Independent PKC-Mediated Phosphorylation of GSK3beta. *Mol Cancer Ther*. 2018;17(1):232-242.
44. Fang X, Yu SX, Lu Y, Bast RC, Jr., Woodgett JR, Mills GB. Phosphorylation and inactivation of glycogen synthase kinase 3 by protein kinase A. *Proc Natl Acad Sci U S A*. 2000;97(22):11960-11965.
45. Liu H, Ai J, Shen A, et al. c-Myc Alteration Determines the Therapeutic Response to FGFR Inhibitors. *Clin Cancer Res*. 2017;23(4):974-984.
46. Sears RC. The life cycle of C-myc: from synthesis to degradation. *Cell Cycle*. 2004;3(9):1133-1137.

47. Biroccio A, Benassi B, Fiorentino F, Zupi G. Glutathione depletion induced by c-Myc downregulation triggers apoptosis on treatment with alkylating agents. *Neoplasia*. 2004;6(3):195-206.
48. Ri M, Iida S, Nakashima T, et al. Bortezomib-resistant myeloma cell lines: a role for mutated PSMB5 in preventing the accumulation of unfolded proteins and fatal ER stress. *Leukemia*. 2010;24(8):1506-1512.
49. Dytfeld D, Luczak M, Wrobel T, et al. Comparative proteomic profiling of refractory/relapsed multiple myeloma reveals biomarkers involved in resistance to bortezomib-based therapy. *Oncotarget*. 2016;7(35):56726-56736.
50. Gorrini C, Harris IS, Mak TW. Modulation of oxidative stress as an anticancer strategy. *Nat Rev Drug Discov*. 2013;12(12):931-947.
51. Gangemi S, Allegra A, Alonci A, et al. Increase of novel biomarkers for oxidative stress in patients with plasma cell disorders and in multiple myeloma patients with bone lesions. *Inflamm Res*. 2012;61(10):1063-1067.
52. Mehdi WA, Zainulabdeen JA, Mehde AA. Investigation of the antioxidant status in multiple myeloma patients: effects of therapy. *Asian Pac J Cancer Prev*. 2013;14(6):3663-3667.
53. Sharma A, Tripathi M, Satyam A, Kumar L. Study of antioxidant levels in patients with multiple myeloma. *Leuk Lymphoma*. 2009;50(5):809-815.
54. Kaiser MF, Johnson DC, Wu P, et al. Global methylation analysis identifies prognostically important epigenetically inactivated tumor suppressor genes in multiple myeloma. *Blood*. 2013;122(2):219-226.
55. Salem K, McCormick ML, Wendlandt E, Zhan F, Goel A. Copper-zinc superoxide dismutase-mediated redox regulation of bortezomib resistance in multiple myeloma. *Redox Biol*. 2015;4:23-33.
56. Chu L, Su MY, Maggi LB, Jr., et al. Multiple myeloma-associated chromosomal translocation activates orphan snoRNA ACA11 to suppress oxidative stress. *J Clin Invest*. 2012;122(8):2793-2806.
57. Moss RW. Should patients undergoing chemotherapy and radiotherapy be prescribed antioxidants? *Integr Cancer Ther*. 2006;5(1):63-82.
58. Hu T, Wu Q, Chong Y, et al. FGFR1 fusion kinase regulation of MYC expression drives development of stem cell leukemia/lymphoma syndrome. *Leukemia*. 2018;32(11):2363-2373.
59. Chen H, Liu H, Qing G. Targeting oncogenic Myc as a strategy for cancer treatment. *Signal Transduct Target Ther*. 2018;3:5.
60. Gao P, Tchernyshyov I, Chang TC, et al. c-Myc suppression of miR-23a/b enhances mitochondrial glutaminase expression and glutamine metabolism. *Nature*. 2009;458(7239):762-765.
61. Bansal A, Simon MC. Glutathione metabolism in cancer progression and treatment resistance. *J Cell Biol*. 2018;217(7):2291-2298.
62. Yuneva M, Zamboni N, Oefner P, Sachidanandam R, Lazebnik Y. Deficiency in glutamine but not glucose induces MYC-dependent apoptosis in human cells. *J Cell Biol*. 2007;178(1):93-105.
63. Holien T, Vatsveen TK, Hella H, Waage A, Sundan A. Addiction to c-MYC in multiple myeloma. *Blood*. 2012;120(12):2450-2453.
64. Kuehl WM, Bergsagel PL. MYC addiction: a potential therapeutic target in MM. *Blood*. 2012;120(12):2351-2352.
65. Shaffer AL, Emre NC, Lamy L, et al. IRF4 addiction in multiple myeloma. *Nature*. 2008;454(7201):226-231.
66. Song IS, Kim HK, Lee SR, et al. Mitochondrial modulation decreases the bortezomib-resistance in multiple myeloma cells. *Int J Cancer*. 2013;133(6):1357-1367.

67. Chng WJ, Huang GF, Chung TH, et al. Clinical and biological implications of MYC activation: a common difference between MGUS and newly diagnosed multiple myeloma. *Leukemia*. 2011;25(6):1026-1035.
68. Cobbold LC, Wilson LA, Sawicka K, et al. Upregulated c-myc expression in multiple myeloma by internal ribosome entry results from increased interactions with and expression of PTB-1 and YB-1. *Oncogene*. 2010;29(19):2884-2891.
69. Dib A, Gabrea A, Glebov OK, Bergsagel PL, Kuehl WM. Characterization of MYC translocations in multiple myeloma cell lines. *J Natl Cancer Inst Monogr*. 2008(39):25-31.
70. Holien T, Misund K, Olsen OE, et al. MYC amplifications in myeloma cell lines: correlation with MYC-inhibitor efficacy. *Oncotarget*. 2015;6(26):22698-22705.

| Pt. | DIAGNOSIS | SEX | AGE | t(4;14) | RESPONSE TO NSC12 | CELL DEATH (%) | | | |
|---|---|---|---|---|---|---|---|---|---|
| | | | | | | DMSO | NSC12 | | |
| | | | | | | | 3 μM | 6 μM | 10 μM |
| 1 | ND | M | 68 | n.d. | yes | 27.2 | - | 91.7 | 94.5 |
| 2 | ND | M | 67 | negative | yes | 15.9 | 21.6 | 23.8 | 73.3 |
| 3 | ND | M | 88 | negative | yes | 14.3 | 16.4 | 37.2 | 85.3 |
| 4 | R/R | F | 67 | negative | yes | 11.5 | 12.4 | 21.1 | 61.7 |
| 5 | ND | F | 64 | positive | yes | 16.0 | 20.4 | 35.5 | 79.9 |
| 6 | R/R | M | 66 | negative | no | 36.0 | 39.9 | 43.5 | 53.5 |
| 7 | R/R | F | 51 | positive | yes | 39.5 | 50.7 | 53.8 | 76.9 |
| 8 | R/R | F | 79 | negative | yes | 44.0 | 49.7 | 54.7 | 68.3 |
| 9 | ND | F | 72 | negative | yes | 30.5 | 36.9 | 83.3 | - |
| 10 | R/R | F | 55 | negative | no | 7.3 | 11.0 | 13.3 | 15.7 |
| 11 | R/R | F | 66 | negative | yes | 21.2 | 37.7 | 46.4 | 46.6 |
| 12 | R/R | M | 51 | negative | yes | 5.3 | 27.5 | 56.4 | 55.0 |
| 13 | ND | M | 45 | negative | yes | 4.3 | 23.5 | 40.6 | 66.1 |
| 14 | R/R | F | 66 | n.d. | no | 31.5 | 24.4 | 27.5 | 23.1 |
| 15 | R/R | F | 64 | negative | yes | 11.0 | 69.3 | 87.8 | 89.3 |
| 16 | ND | M | 64 | negative | yes | 20.7 | 25.8 | 34.8 | 52.4 |
| 17 | ND | M | 53 | n.d. | yes | 3.7 | 7.4 | 25.1 | 91.2 |
| 18 | R/R | M | 57 | n.d. | yes | 5.1 | 21.7 | 22.7 | 63.5 |
| 19 | R/R | F | 73 | n.d. | yes | 26.6 | 35.7 | 46.0 | 64.2 |
| 20 | ND | F | 68 | n.d. | yes | 5.0 | 12.0 | 32.6 | 83.8 |
| 21 | R/R | M | 73 | n.d. | yes | 2.9 | 5.9 | 25.1 | 76.3 |
| 22 | R/R | M | 75 | n.d. | yes | 7.7 | 12.2 | 31.4 | 87.4 |
| 23 | R/R | M | 65 | negative | yes | 31.9 | - | - | 68.6 |
| 24 | R/R | M | 69 | negative | yes | 25.6 | - | - | 57.3 |
| 25 | R/R | F | 65 | positive | no | 10.8 | - | - | 21.9 |
| 26 | ND | M | 61 | n.d. | yes | 31.3 | - | - | 71.6 |

**Table 1. Patient-derived MM cells treated with NSC12.** Individual response of patient-derived MM cells to NSC12 treatment. Data are the mean of three replicates.
ND: Newly Diagnosed; R/R: Relapsed/Refractory; n.d.: not determined.

**FIGURE LEGENDS**

**Figure 1. *In vitro* effects of FGF blockade in MM cells.**

(A) Viable cell counts by cytofluorimetric analysis of MM cell lines harbouring or not the t(4;14) and treated with NSC12 for 72 hours. Data are mean ± SEM.

(B) Cell cycle analysis of MM cell lines harbouring or not the t(4;14) and treated with NSC12 for 72 hours. Data are mean ± SEM. **$p < 0.01$, #$p < 0.001$.

(C) Cytofluorimetric analysis of apoptotic cell death of t(4;14)-positive KMS-11 and t(4;14)-negative RPMI8226 cells after treatment with NSC12 6 μM.

(D) Western blot analysis of KMS-11 and RPMI8226 cells after treatment with NSC12 6 μM.

**Figure 2. FGF trapping inhibits MM growth *in vivo*.**

(A) Analysis of phospho-FGFR3 levels by immunofluorescence (left panel) and western blot (right panels) in s.c. KMS-11 alginate plugs after 4-days oral treatment with NSC12 7.5 mg/Kg (n= 4 mice/group). pFGFR3/FGFR3 densitometry was quantified with ImageJ software and normalized to β-actin. Scale bar 100 μm.

(B) Tumor growth of KMS-11 and RPMI8226 cells injected s.c. and orally treated (arrows) with NSC12 or vehicle (n = 10 mice/group).

(C) Immunohistochemical analysis of KMS-11 and RPMI8226 tumors harvested at the end of the experiment described in (B). Quantification of pHH3- and TUNEL-positive cells was carried out by ImageJ software. Scale bar 50 μm.

Data are mean ± SEM. In box and whiskers graphs, boxes extend from the $25^{th}$ to the $75^{th}$ percentiles, lines indicate the median values, and whiskers indicate the range of values.

*$p < 0.05$, #$p < 0.001$.

**Figure 3. FGF inhibition hampers MM dissemination.**

(A) Western blot analysis of phospho-FGFR1 and phospho-FGFR3 levels in MM.1S cells treated with NSC12 6 μM.

(B) Viable cell counts and apoptotic cell death by cytofluorimetric analysis of NSC12-treated MM.1S cells.

(C) Quantification of MM.1S cells migrated towards chemotactic stimuli in a chemiotaxis assay.

(D) Western blot analysis of phospho and total FAK, and β-catenin levels in MM.1S cells treated with NSC12 6 μM.

(E-F) DMSO- or NSC12-treated MM.1S cells (6 μM for 3 hours) were stained with red or blue fluorescent dye, respectively, injected in the Zebrafish Cuvier Duct and assessed for their ability to migrate to the zebrafish caudal hematopoietic tissue (CHT) (E). Fluorescent area of MM.1S cells inside or outside the CHT were quantified by ImageJ software (F). (n = 33 zebrafish embryos/group).

(G) Cytofluorimetric analysis of BM colonization by GFP/Luciferase-expressing MM.1S eight weeks after i.v. injection in SCID beige mice.

(H) GFP/Luciferase-expressing MM.1S cells were injected i.v. in SCID beige mice; when 10-20% of BM disease infiltration was achieved, mice received a 3-days course of NSC12 treatment and western blot analysis of BM lysates after femur flushing was performed. (n = 3 mice/group).

(I) SCID beige mice were injected i.v. with GFP/Luciferase-expressing MM.1S cells and treated every other day for 4 weeks with NSC12 7.5 mg/Kg or vehicle (n = 12 mice/group). Bioluminescence imaging (left panel) and quantification (right panel) of luciferase-expressing MM.1S cells are shown.

Data are mean ± SEM. *$p < 0.05$, #$p < 0.001$.

**Figure 4. FGF inhibition induces oxidative stress-mediated apoptosis in MM cells.**

(A) Vulcano plot (left panel) and hierarchical clustering (right panel) of $Log_2$ 2-fold differentially expressed genes ($p < 0.01$) in KMS-11 cells treated with NSC12 6 μM for 12 hours.

(B) Cytofluorimetric analysis of mtROS production (Mitosox) and mitochondrial membrane depolarization (TMRE) in NSC12-treated KMS-11 cells.

(C) Western blot analysis of PARP inactivation and phospho-H2AX (γH2AX) expression in KMS-11 cells treated with NSC12 6 μM.

(D) Analysis of mitochondrial activity by Seahorse assay for oxygen consumption rate (OCR) in KMS-11 cells treated with NSC12 6 μM.

(E) Anti-nitro tyrosine and anti-pH2AX staining of s.c. KMS-11 and RPMI8226 tumors grown in NSC12- or vehicle-treated mice (n = 5 mice/group). Scale bar 50 μm.

(F-G) Cytofluorimetric (F) and western blot analyses (G) of KMS-11 cells treated with NSC12 6 μM for 12 hours in the presence or absence of Vitamin E.

Data are mean ± SEM. #$p < 0.001$.

**Figure 5. Oxidative stress-induced apoptosis following FGF inhibition is c-Myc-dependent.**

(A) Gene Set Enrichment Analysis (GSEA) for c-Myc targets in KMS-11 cells treated with NSC12 6 μM for 12 hours.

(B) Western blot analysis of KMS-11 cells treated with NSC12 6 μM (upper panel) and KMS-11 s.c. tumors (lower panel) grown in NSC12- or vehicle-treated mice.

(C) Western blot analysis of c-Myc levels in KMS-11 cells treated with NSC12 6 μM for 3 hours in the presence or absence of the proteasome inhibitor MG132.

(D) Western blot analysis of c-Myc levels in WT and $Myc^{(T58A)}$ mutant KMS-11 cells treated with NSC12 6 μM for 3 hours.

(E) Cytofluorimetric analysis of mtROS production and apoptotic cell death in WT and $Myc^{(T58A)}$ mutant KMS-11 cells after 12 hours of NSC12 treatment.

(F) Cytofluorimetric analysis of intracellular GSH content in KMS-11 cells after treatment with NSC12 6 μM.

(G) Cytofluorimetric analysis of intracellular GSH content in WT and $Myc^{(T58A)}$ mutant KMS-11 cells treated with NSC12 6 μM for 12 hours. Values of GSH median fluorescence intensity are reported in the histogram plot.

(H) Cytofluorimetric analysis of intracellular GSH content in KMS-11 cells treated with NSC12 6 μM for 12 hours in the presence or absence of Vitamin E.

Data are mean ± SEM. *$p < 0.05$, #$p < 0.001$.

**Figure 6. Effect of FGF trapping in patient-derived MM cells.**

(A) Analysis of patient-derived MM cell death after 12 hours of treatment with increasing doses of NSC12. Only NSC12 responsive MM cases are reported (22 cases out of 26). PBMCs were tested as control. Each dot represents a single MM case or PBMC isolate, and lines indicate the mean values (n = 26 MM cases; n = 8 PBMC isolates).

(B-C) Western blot analysis of MM cells purified from newly diagnosed (naïve) and relapsed/refractory patients and treated with NSC12 for 12 hours; GAPDH was probed for loading control (n = 3 MM cases). GAPDH image for pts. 4 and 5 are the same in B and C since obtained from the same blot.

(D) qPCR analysis for the expression levels of oxidative-stress induced genes in patient-derived MM cells treated with NSC12 6 μM for 6 hours (n = 3 MM cases).

(E) Immunofluorescence analysis and quantification of patient-derived MM cells treated with NSC12 6 μM for 12 hours (n = 2 MM cases). Scale bar 20 μm.

(F) Cytofluorimetric analysis of patient-derived MM cells treated with NSC12 10 μM for 12 hours in the presence or absence of Vitamin E (n = 3 MM cases).

Data are mean ± SEM. #$p < 0.001$.

**Figure 7. Resistance to Bortezomib does not affect the antitumor activity of FGF blockade.**

(A) MM cells purified from naïve or refractory/relapsed patients were treated with NSC12 10 μM for 12 hours and cell death assessed by cytofluorimetric analysis (n = 26 MM cases).

(B) Bortezomib-resistant (KMS-11/BTZ) or parental KMS-11 cells were treated with increasing doses of BTZ or NSC12 for 48 hours and assessed for viable cell counting by cytofluorimetric analysis.

(C) Western blot analysis of KMS-11/BTZ cells treated with NSC12 6 μM.

(D) Cytofluorimetric analysis of mtROS production (MitoSox), mitochondrial membrane depolarization (TMRE) and apoptotic cell death in KMS-11/BTZ cells treated with NSC12 6 μM.

(E) Tumor growth (right panel) and tumor weight (left panel) of KMS-11/BTZ cells grafted s.c and orally treated (arrows) with NSC12 or vehicle (n = 5 mice/group).

(F) qPCR analysis for the expression levels of TXNCD5 and PRDX3 genes in parental and BTZ-resistant KMS-11 cells treated with NSC12 6 μM.

Data are mean ± SEM. In box and whiskers graphs, boxes extend from the $25^{th}$ to the $75^{th}$ percentiles, lines indicate the median values, and whiskers indicate the range of values.

*$p < 0.05$, **$p < 0.01$, #$p < 0.001$.

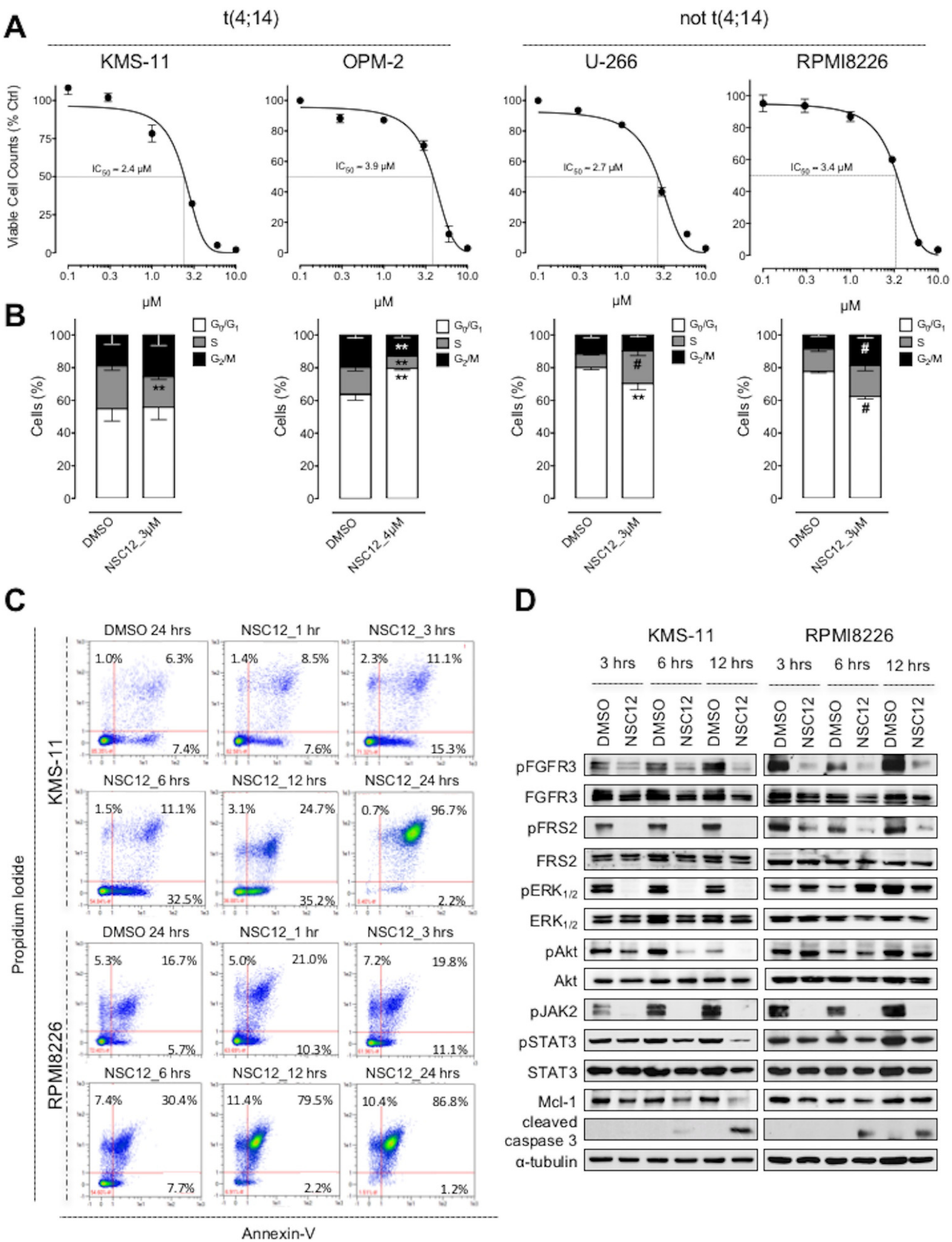
A
t(4;14)
not t(4;14)
KMS-11
OPM-2
U-266
RPMI8226
Viable Cell Counts (% Ctrl)
IC50 = 2.4 μM
IC50 = 3.9 μM
IC50 = 2.7 μM
IC50 = 3.4 μM
μM
B
Cells (%)
G0/G1
S
G2/M
DMSO
NSC12_3μM
NSC12_4μM
C
KMS-11
RPMI8226
DMSO 24 hrs
NSC12_1 hr
NSC12_3 hrs
NSC12_6 hrs
NSC12_12 hrs
NSC12_24 hrs
Propidium Iodide
Annexin-V
D
KMS-11
RPMI8226
3 hrs
6 hrs
12 hrs
DMSO
NSC12
pFGFR3
FGFR3
pFRS2
FRS2
pERK1/2
ERK1/2
pAkt
Akt
pJAK2
pSTAT3
STAT3
Mcl-1
cleaved caspase 3
α-tubulin

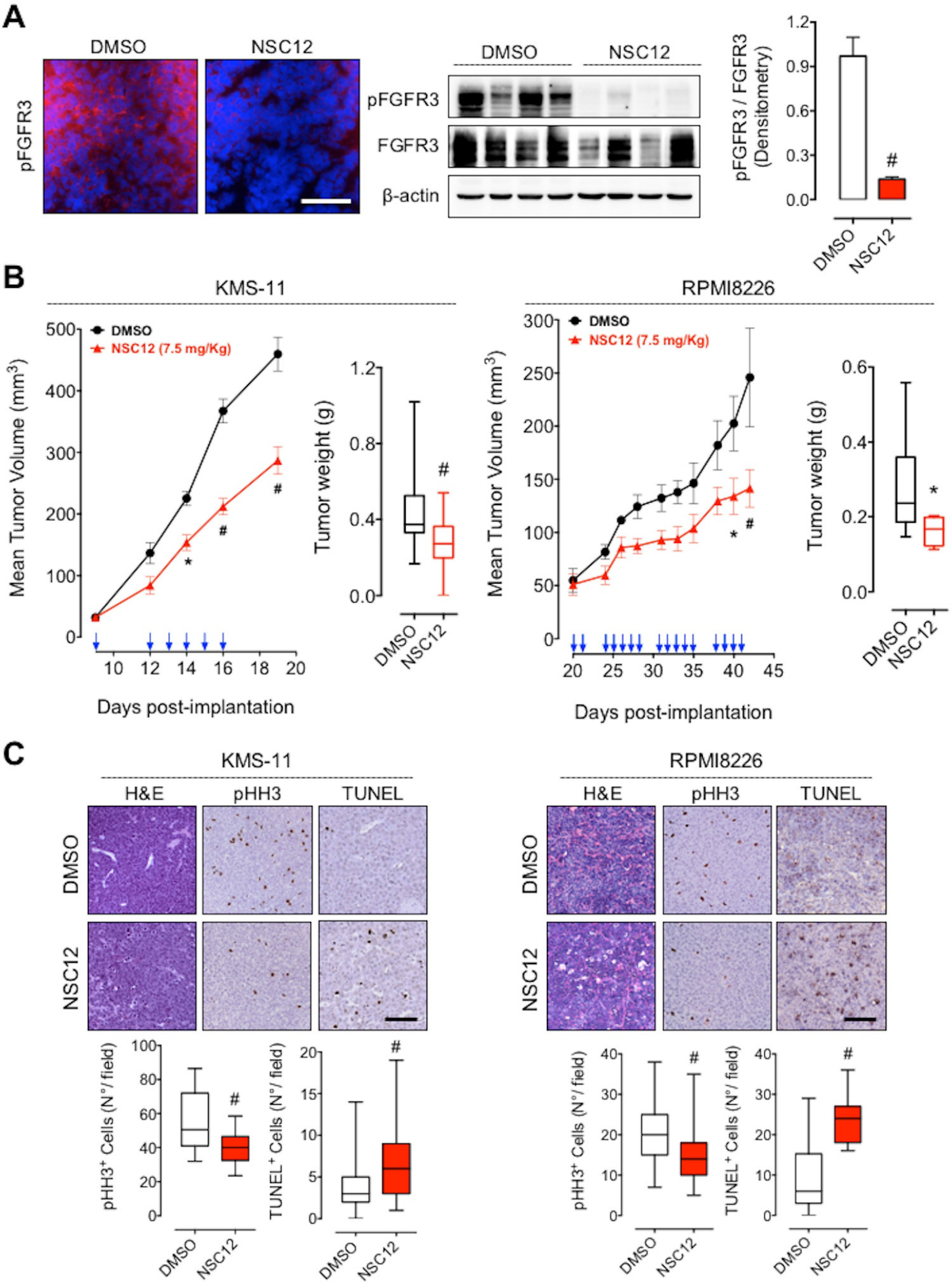
A
DMSO
NSC12
pFGFR3
pFGFR3
FGFR3
β-actin
pFGFR3 / FGFR3 (Densitometry)
B
KMS-11
RPMI8226
DMSO
NSC12 (7.5 mg/Kg)
Mean Tumor Volume (mm3)
Days post-implantation
Tumor weight (g)
C
H&E
pHH3
TUNEL
pHH3+ Cells (N°/ field)
TUNEL+ Cells (N°/ field)

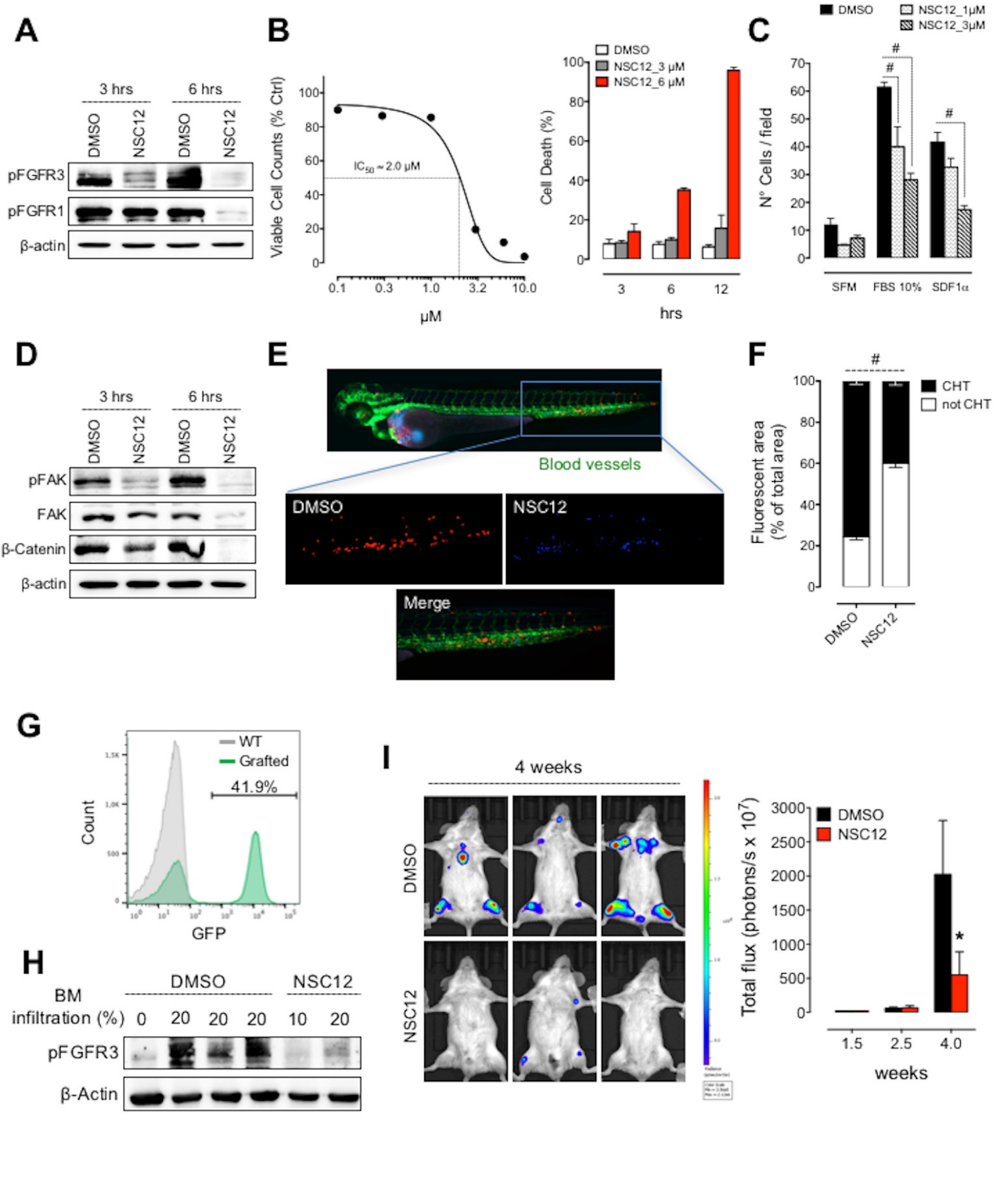
A
3 hrs
6 hrs
DMSO
NSC12
DMSO
NSC12
pFGFR3
pFGFR1
β-actin
B
Viable Cell Counts (% Ctrl)
IC50 ~ 2.0 μM
μM
DMSO
NSC12_3 μM
NSC12_6 μM
Cell Death (%)
hrs
C
DMSO
NSC12_1μM
NSC12_3μM
N° Cells / field
SFM
FBS 10%
SDF1α
D
3 hrs
6 hrs
DMSO
NSC12
DMSO
NSC12
pFAK
FAK
β-Catenin
β-actin
E
Blood vessels
DMSO
NSC12
Merge
F
CHT
not CHT
Fluorescent area (% of total area)
DMSO
NSC12
G
WT
Grafted
41.9%
Count
GFP
H
BM infiltration (%)
DMSO
NSC12
0
20
20
20
10
20
pFGFR3
β-Actin
I
4 weeks
DMSO
NSC12
DMSO
NSC12
Total flux (photons/s x 10^7)
weeks

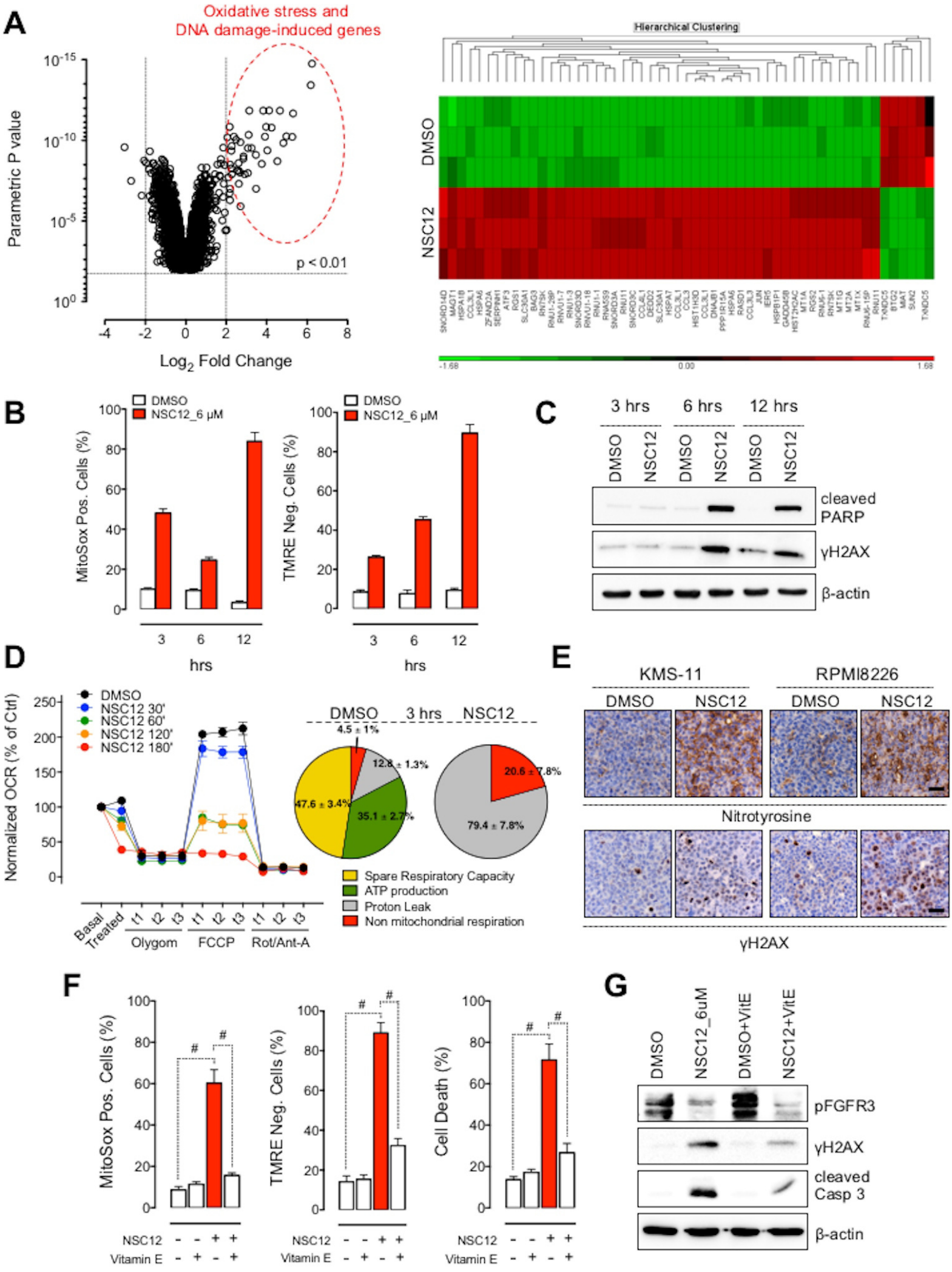
A
Oxidative stress and
DNA damage-induced genes
Parametric P value
Log2 Fold Change
p < 0.01
Hierarchical Clustering
DMSO
NSC12
B
DMSO
NSC12_6 μM
MitoSox Pos. Cells (%)
TMRE Neg. Cells (%)
hrs
C
3 hrs
6 hrs
12 hrs
DMSO
NSC12
cleaved PARP
γH2AX
β-actin
D
Normalized OCR (% of Ctrl)
DMSO
NSC12 30'
NSC12 60'
NSC12 120'
NSC12 180'
Basal
Treated
Olygom
FCCP
Rot/Ant-A
DMSO 3 hrs NSC12
4.5 ± 1%
12.8 ± 1.3%
47.6 ± 3.4%
35.1 ± 2.7%
20.6 ± 7.8%
79.4 ± 7.8%
Spare Respiratory Capacity
ATP production
Proton Leak
Non mitochondrial respiration
E
KMS-11
RPMI8226
DMSO
NSC12
Nitrotyrosine
γH2AX
F
MitoSox Pos. Cells (%)
TMRE Neg. Cells (%)
Cell Death (%)
NSC12
Vitamin E
G
DMSO
NSC12_6uM
DMSO+VitE
NSC12+VitE
pFGFR3
γH2AX
cleaved Casp 3
β-actin

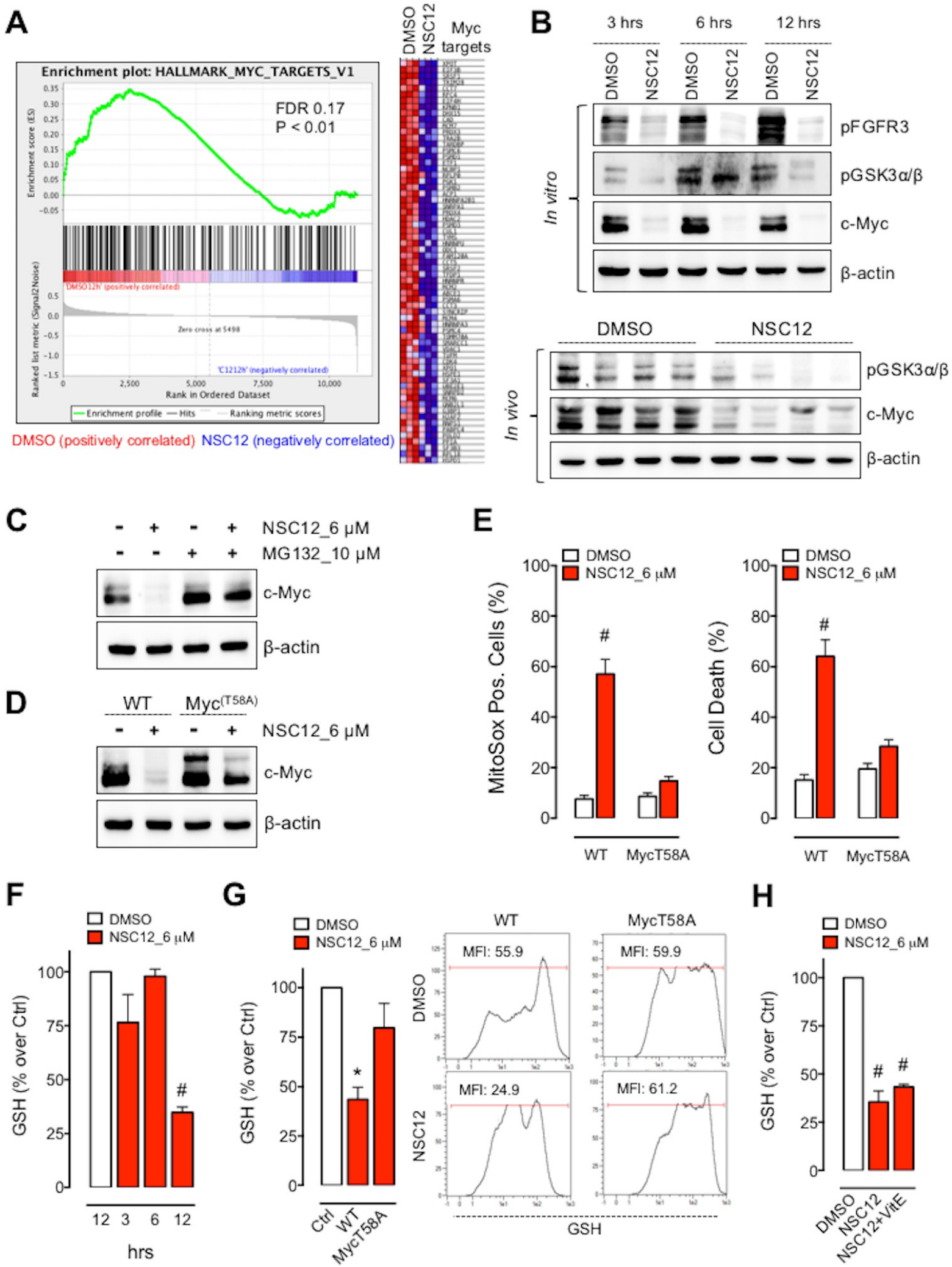
A
Enrichment plot: HALLMARK_MYC_TARGETS_V1
FDR 0.17
P < 0.01
Enrichment score (ES)
Ranked list metric (Signal2Noise)
'DMSO12h' (positively correlated)
Zero cross at 5498
'C1212h' (negatively correlated)
Rank in Ordered Dataset
Enrichment profile
Hits
Ranking metric scores
DMSO
NSC12
Myc targets
DMSO (positively correlated) NSC12 (negatively correlated)
B
3 hrs
6 hrs
12 hrs
DMSO
NSC12
pFGFR3
pGSK3α/β
c-Myc
β-actin
In vitro
In vivo
C
NSC12_6 μM
MG132_10 μM
c-Myc
β-actin
D
WT
Myc(T58A)
NSC12_6 μM
c-Myc
β-actin
E
DMSO
NSC12_6 μM
MitoSox Pos. Cells (%)
Cell Death (%)
WT
MycT58A
F
GSH (% over Ctrl)
hrs
G
WT
MycT58A
MFI: 55.9
MFI: 59.9
MFI: 24.9
MFI: 61.2
GSH
H
DMSO
NSC12
NSC12+VitE

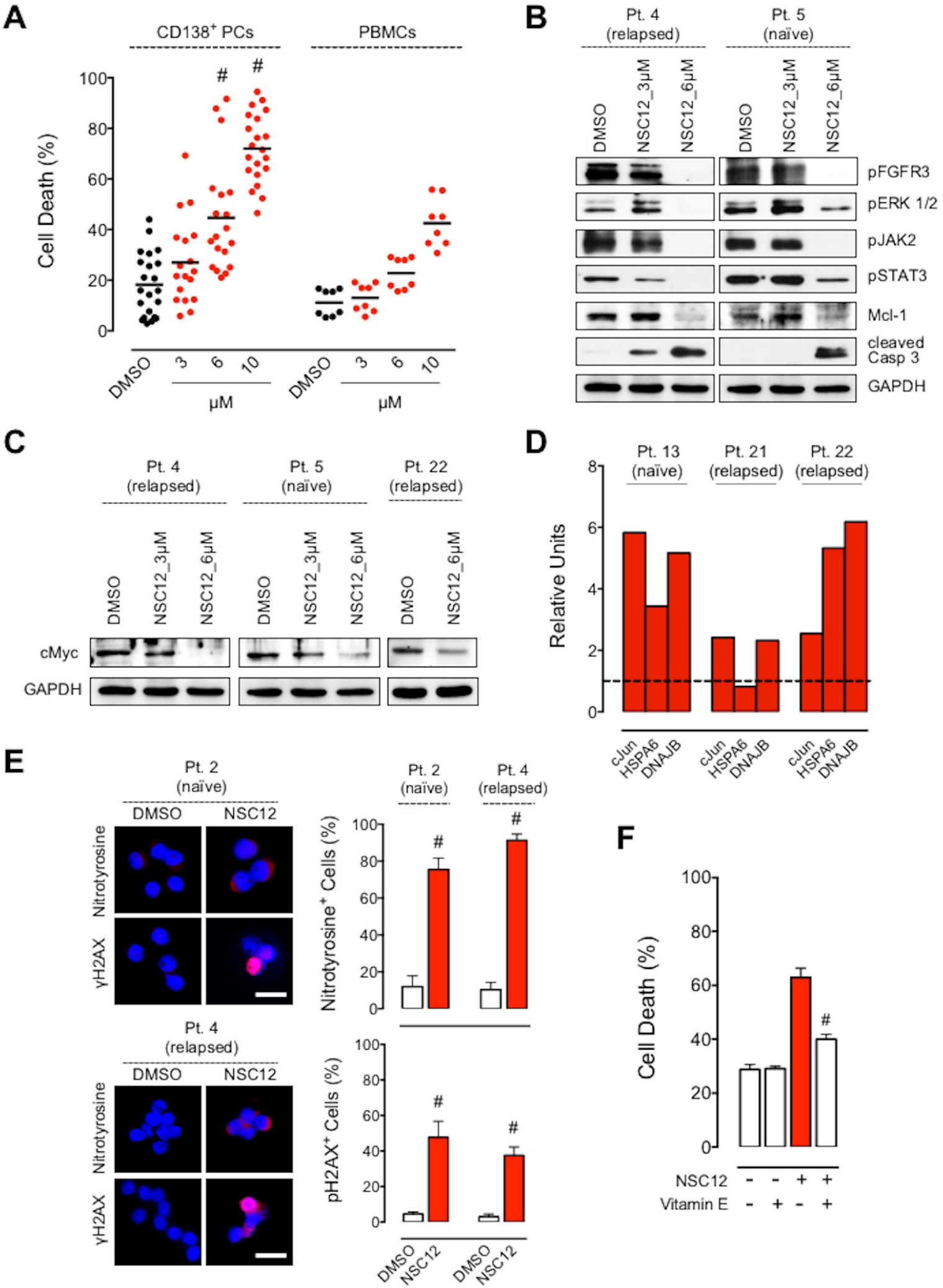
A
CD138+ PCs
PBMCs
Cell Death (%)
DMSO
3
6
10
μM
B
Pt. 4 (relapsed)
Pt. 5 (naïve)
DMSO
NSC12_3μM
NSC12_6μM
pFGFR3
pERK 1/2
pJAK2
pSTAT3
Mcl-1
cleaved Casp 3
GAPDH
C
Pt. 4 (relapsed)
Pt. 5 (naïve)
Pt. 22 (relapsed)
cMyc
GAPDH
D
Pt. 13 (naïve)
Pt. 21 (relapsed)
Pt. 22 (relapsed)
Relative Units
cJun
HSPA6
DNAJB
E
Pt. 2 (naïve)
Pt. 4 (relapsed)
DMSO
NSC12
Nitrotyrosine
γH2AX
Nitrotyrosine+ Cells (%)
pH2AX+ Cells (%)
F
Cell Death (%)
NSC12
Vitamin E

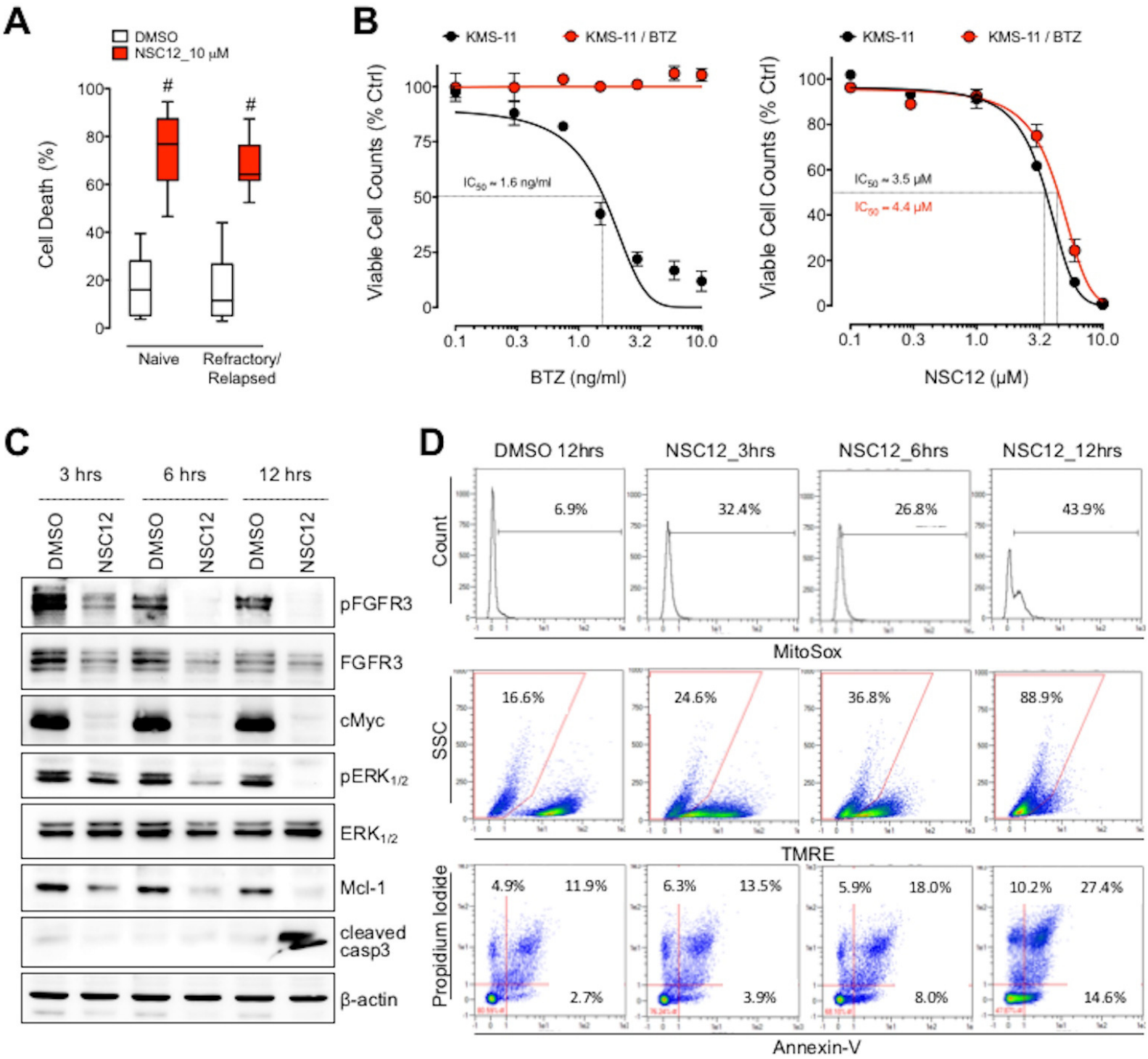
A
DMSO
NSC12_10 μM
Cell Death (%)
Naive
Refractory/ Relapsed
B
KMS-11
KMS-11 / BTZ
Viable Cell Counts (% Ctrl)
IC50 ~ 1.6 ng/ml
BTZ (ng/ml)
IC50 ~ 3.5 μM
IC50 ~ 4.4 μM
NSC12 (μM)
C
3 hrs
6 hrs
12 hrs
DMSO
NSC12
pFGFR3
FGFR3
cMyc
pERK1/2
ERK1/2
Mcl-1
cleaved casp3
β-actin
D
DMSO 12hrs
NSC12_3hrs
NSC12_6hrs
NSC12_12hrs
Count
6.9%
32.4%
26.8%
43.9%
MitoSox
SSC
16.6%
24.6%
36.8%
88.9%
TMRE
Propidium Iodide
4.9%
11.9%
2.7%
6.3%
13.5%
3.9%
5.9%
18.0%
8.0%
10.2%
27.4%
14.6%
Annexin-V
E
DMSO
NSC12 (7.5 mg/Kg)
Tumor volume (mm3)
Days post-implantation
Tumor weight (g)
DMSO
NSC12
F
KMS-11
KMS-11/BTZ
PRDX3
TXNDC5
Relative Units
hrs